

- ¹⁰A. M. Lane and R. G. Thomas, *Rev. Mod. Phys.* **30**, 257 (1958).
- ¹¹T. A. Tombrello, *Phys. Rev.* **143**, 609 (1966).
- ¹²D. H. McSherry and S. D. Baker, *Phys. Rev. C* **1**, 888 (1970).
- ¹³P. Szydlik and C. Werntz, *Phys. Rev.* **138**, B866 (1964).
- ¹⁴B. H. Bransden, H. H. Robertson, and P. Swan, *Proc. Phys. Soc. (London)* **69A**, 601 (1956).
- ¹⁵R. Seki and Z. Cromer, *Phys. Rev.* **156**, 93 (1967).
- ¹⁶R. Wetmore, D. Buckle, J. Kane, and R. Siegel, *Phys. Rev. Letters* **19**, 1003 (1967).
- ¹⁷K. A. Brueckner, *Phys. Rev.* **98**, 769 (1955).
- ¹⁸B. R. Barrett, *Phys. Rev.* **154**, 955 (1966).
- ¹⁹G. Sh. Gogsadze and T. I. Kopsleishvili, *Yadern. Fiz.* **8**, 875 (1968) [transl.: *Soviet J. Nucl. Phys.* **8**, 509 (1969)].
- ²⁰The instrumental resolution function for this experiment was kindly supplied to us by Dr. P. Truol.
- ²¹M. Ericson and T. E. O. Ericson, *Ann. Phys. (N.Y.)* **36**, 323 (1966).
- ²²S. Berezin, G. Burleson, D. Eartly, A. Roberts, and T. O. White, *Phys. Letters* **30B**, 27 (1969).
- ²³D. Jenkins and R. Kunselman, *Phys. Rev. Letters* **17**, 1148 (1968).
- ²⁴D. R. Thompson, *Nucl. Phys.* **A154**, 442 (1970).
- ²⁵S. Skupsky, *Phys. Letters* **36B**, 271 (1971).

Clustering Characteristics of ${}^6\text{Li}$ from the ${}^6\text{Li}(\alpha, \alpha x)Y$ Reaction at $E_\alpha = 50$ MeV

J. M. Lambert,* R. J. Kane,† P. A. Treado,* L. A. Beach, E. L. Petersen, and R. B. Theus
U. S. Naval Research Laboratory, Washington, D. C. 20390

(Received 19 August 1971)

The quasielastic scattering of 50-MeV α particles has been used as a tool to study the cluster configurations of the ${}^6\text{Li}$ nucleus by means of the ${}^6\text{Li}(\alpha, \alpha x)Y$ reaction. Data have been obtained in kinematically complete experiments and at exact quasielastic angles for those cases corresponding to $x = p, d, t, {}^3\text{He}$, and α . Analysis has been carried out in the framework of the plane-wave impulse approximation. Quasielastic cross sections have been measured and experimental momentum distributions extracted. Theoretical fits to these distributions using simple Gaussian and exponential functions have been calculated and used to determine both absolute and relative clustering probabilities with fair success. The more reliable relative probabilities indicate strong p, d , and α clustering in ${}^6\text{Li}$ and rather weak t and ${}^3\text{He}$ clustering.

I. INTRODUCTION

Multiparticle-breakup (MPB) reaction studies have expanded substantially in recent years and have provided a useful method of investigating nuclear structure and reactions.¹⁻³ Present detection and analysis techniques identify particles and record coincident energy information for numerous outgoing channels in kinematically complete experiments involving more than two particles in the final state. For relatively low bombarding energies, this type of experiment has been shown to proceed by sequential-decay processes through definite states of particle-unstable systems.⁴⁻⁷ For moderate bombarding energies, the "quasi-elastic" (QE) process has been observed and studied.⁸⁻¹⁰ In this process, it is assumed that the target nucleus has a structure consisting of identifiable nucleons and/or clusters of nucleons, and that the nucleons or clusters can be knocked out of the system in a manner that can be described in terms of elastic scattering of the incident particle and the product particle or cluster. Reac-

tions such as $(p, 2p)$, $(\alpha, 2\alpha)$, and $(p, p\alpha)$ typify this process.

The techniques of MPB, in general, and QE scattering, in particular, should be very useful for investigating questions relating to the cluster and shell models of nuclei, even though the interpretation of such experiments is difficult and still debated.¹¹ Some of the early QE experiments suggested that in the $(p, 2p)$ process it was possible to knock out protons with different binding energies that were interpreted as being associated with different shells of the nucleus.^{12,13} In addition, angular-distribution studies indicated that angular momentum information about the target nucleus could be obtained.^{14,15} This information suggested that the shell model may not be valid for the ${}^6\text{Li}$ nucleus.¹⁶ Previous experiments have investigated a given QE process, for example $(\alpha, 2\alpha)$, using various targets to determine the validity of the assumptions used in the analysis of such experiments. The validity of the plane-wave impulse approximation¹⁷ (PWIA), the use of a modified cutoff approximation,¹⁸ the separa-

bility of the cross sections in terms of free elastic cross sections,¹⁹ and the question of what is the appropriate energy for "off-the-energy-shell" approximations²⁰ have been discussed.

This experiment was performed to utilize the QE process as a tool, rather than to investigate the process; the purpose was to determine the cluster configurations that could be observed in a given nucleus. The nucleus ${}^6\text{Li}$ was examined because of the relative simplicity of the possible cluster configurations. A search for p , d , t , ${}^3\text{He}$, and α clustering was accomplished by measuring the cross sections for the ${}^6\text{Li}(\alpha, \alpha x)Y$ reactions with $x=p$, d , t , ${}^3\text{He}$, and α . Since ${}^5\text{He}$ is unstable, no attempt was made to observe it, but the data from the $(\alpha, \alpha p)$ reaction furnish the appropriate information on that clustering possibility. The experiments were performed with the restriction that the unobserved particle or cluster in each case must be in its ground state and must be at rest for some point on the kinematic locus. For every angle pair used, a portion of the locus corresponding to the appropriate QE process was identified. Preliminary results of this work have been presented at an American Physical Society meeting.¹¹

II. QUASIELASTIC SCATTERING PROCESS

Analysis of previous $(p, 2p)$ experiments¹²⁻¹⁵ has led to a questioning of the validity of the shell model for low- A nuclei, particularly ${}^6\text{Li}$. The first experimental data¹² suggested that the least tightly bound proton in ${}^6\text{Li}$ was bound in an $l=0$ orbital. This interpretation of the data was later proven to be false using quite general arguments.²¹ Subsequent analysis of these and similar data and comparisons with theory have led to contradictions indicating a quantitative breakdown of the shell model for ${}^6\text{Li}$.^{14, 22, 23} The QE process should provide a valuable method for further elucidating such problems of nuclear structure.

The cross section for quasielastic scattering in the plane-wave Born approximation has the form²⁴

$$\frac{d^3\sigma}{d\Omega_1 d\Omega_2 dE_1} \propto \rho \frac{d\sigma}{d\Omega_f} |\Phi(q)|^2; \quad (1)$$

where ρ is the phase-space factor; $d\sigma/d\Omega_f$ is the c.m. differential cross section for free 1-2 scattering; and $|\Phi(q)|^2$ is the probability that the spectator (3) has momentum q , given by the square of the absolute value of the Fourier transform of the spatial distribution of the spectator in the target. The appropriate energy to use in selecting the free scattering cross section is in question,¹⁹ and can range between the initial- and final-state relative energies of the scattering particles. A recent experiment indicates that in the case of $(\alpha, 2\alpha)$

scattering the free cross section corresponding to the final-state relative energy should be used.²⁵

This was shown when a very sharp resonance in the free α - α cross section was observed for a final-state relative energy equivalent to this resonance energy, but not for an energy corresponding to the initial-state relative energy. Experiments on other reactions have not been successfully analyzed by using the final-state relative energy.²⁶

III. EXPERIMENTAL APPARATUS AND PROCEDURES

A. Targets and Scattering Chamber

The 50-MeV analyzed α -particle beam from the Naval Research Laboratory cyclotron was used to bombard 99.4% isotopically enriched Li targets of LiF with Mylar backings. An ORTEC 76-cm-diam scattering chamber was used with a 0.95-cm-diam halo entrance aperture, and the beam was collected in a Faraday cup approximately 4 m downstream from the target. The beam was aligned and checked periodically by means of a small aperture in place of the target.

B. Detection System

Two Si surface-barrier detector telescopes and associated electronics, which includes two particle identifiers, a coincidence-event selection circuit, and an on-line EMR 6050 computer, comprise the data accumulation system. Transmission-mounted detectors in ΔE - E arrays in conjunction with particle identifiers were used for detecting protons, deuterons, tritons, ${}^3\text{He}$, and α particles from each of the telescopes. The telescopes had an 0.32-cm-wide by 0.64-cm-high aperture in front, and the thicknesses of the ΔE and E detectors were 27 or 50 μ and 4000 μ , respectively.

These detector telescopes, biased for total depletion of each detector, were utilized with standard coincidence electronics. The resolving time for the system was approximately 50 nsec, assuring detection of only those pulses occurring in one rf cycle of the cyclotron. Accidental events were decreased by pre gating the analog signals to the particle-identifier units. The accidental spectra were measured by inserting a two-rf-cycle time delay in one logic leg and using a second (accidental) coincidence arrangement to tag these events for magnetic-tape storage.

Data for the $(\alpha, \alpha x)$ reactions studied were accumulated in a two-parameter mode with α energy on the x axis, cluster energy on the y axis, and counts on the z axis. Events from the QE and sequential processes are on the kinematic locus

TABLE I. Experimental parameters for the quasielastic scattering reactions studied.

Reaction	$\theta_{\text{lab}} (\alpha)$ (deg)	$\theta_{\text{lab}} (\text{cluster})$ (deg)	$d\sigma/d\Omega$ (elastic) (mb/sr)	$d^3\sigma/d\Omega^2 dE$ (QE) (mb/sr ² MeV)
${}^6\text{Li}(\alpha, 2\alpha){}^2\text{H}$	44.0	44.1	220 ^a	110 ± 33
${}^6\text{Li}(\alpha, \alpha d){}^4\text{He}$	17.5	59.2	30 ^b	13 ± 4
${}^6\text{Li}(\alpha, \alpha {}^3\text{He}){}^3\text{H}$	22.6	22.3	10 ^c	0.7 ± 0.3
${}^6\text{Li}(\alpha, \alpha t){}^3\text{He}$	22.6	22.3
${}^6\text{Li}(\alpha, \alpha p){}^3\text{He}$	10.4	28.7	50 ^d	4.5 ± 2
	10.4	36.1	86 ^d	5. ± 2
	10.0	39.3	125 ^d	12 ± 5

^a H. E. Conzett, G. Igo, H. C. Shaw, and R. J. Slobodrian, Phys. Rev. **117**, 1075 (1960).

^b W. T. H. van Oers and K. W. Brockman, Jr., Nucl. Phys. **44**, 546 (1963).

^c C. G. Jacobs and R. E. Brown, Phys. Rev. C **1**, 1615 (1970).

^d A. C. L. Barnard, C. M. Jones, and J. L. Weil, Nucl. Phys. **50**, 604 (1964).

for the specific three-body breakup of interest. Data along the locus projected on the x axis or y axis provide detailed information about the exit-channel particles. It was typically the case that no background due to accidental events was present under any of the loci of interest. Frequently, however, the loci had sequential-process structure which had to be subtracted. This structure, however, was usually quite small in comparison to the data of interest. During data accumulation the spectral information was tagged by the coincidence-event selection circuit and was stored on magnetic tape in the resolution of 1024 by 1024, while the most important tagged spectrum was monitored with a 64-by-64 scope display. The coincidence-event selection could accommodate up to 16 types of events. All accumulated data were called back from the tape off line in any 2^n by 2^m array where $n + m$ was less than or equal to 13. This technique provided sufficient resolution for the data analysis.

C. Spectra

Coincidence spectra for the set of angle pairs given in Table I were obtained. A monitor detector at 165° was used throughout the experiment to provide a measure of the target deterioration, which was minimal. It should be noted that the angle pairs selected caused the structure due to sequential-decay processes to move continuously in a predictable manner; hence, providing a facility for identification of the spectral contents.

Energy calibration of the total system was accomplished by utilizing the two-body reactions ${}^7\text{Li}(p, \alpha){}^4\text{He}$, ${}^6\text{Li}(p, {}^3\text{He}){}^4\text{He}$, ${}^7\text{Li}(p, d){}^6\text{Li}(\text{g.s.})$, $\text{H}(p, p)\text{H}$, and $\text{H}(\alpha, \alpha)\text{H}$ with coincidence and particle-identification requirements. This technique allowed a simultaneous calibration of both axes, and since the background was nonexistent, calibration points were easy to obtain.

IV. EXPERIMENTAL RESULTS

For each of the QE scattering experiments, ${}^6\text{Li}(\alpha, \alpha x)Y$, a three-body final state exists which is represented by a kinematic locus. Identification of two of the three particles provides a kinematically complete experiment.¹ In each case, angles were chosen so that some part of the locus would correspond to the condition that Y have zero kinetic energy in the laboratory system. An example of the results is most easily discussed in terms of the reaction ${}^6\text{Li}(\alpha, 2\alpha){}^2\text{H}$. Figure 1 shows the kinematic locus for lab angles of $\theta_{\alpha_1} = 44.1^\circ$, $\theta_{\alpha_2} = 44.0^\circ$ giving 90° scattering in the c.m. system. The QE condition of $E_d = 0$ is indicated on the locus, as well as the positions of nearby sequential states. Figure 2(a) shows the projection of that portion of the locus and exhibits a QE peak in good agreement with previous results.^{20, 27-29} This peak has a shape indicating a relative angular momentum of $l=0$ for the x - Y cluster (in this case, α and d).

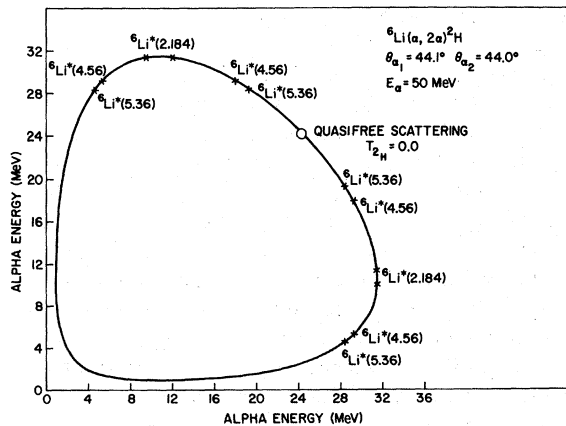


FIG. 1. Kinematic locus for the ${}^6\text{Li}(\alpha, 2\alpha){}^2\text{H}$ reaction at lab angles $\theta_{\alpha_1} = 44.1^\circ$ and $\theta_{\alpha_2} = 44.0^\circ$. Indicated on the locus are the QE condition of $T_d = 0$ as well as the positions of possible sequential states.

It is also possible to have QE scattering for $l \neq 0$, and this is illustrated by Fig. 2(b) showing the results of ${}^7\text{Li}(\alpha, 2\alpha){}^3\text{H}$ with $l=1$. In this case, the typical double-peaked structure has a minimum at the QE position indicating the relative motion of the α - t clusters. This double peaking may indicate a measure of the cluster separation $R_{\alpha-t}$. If the ${}^7\text{Li}(\alpha, 2\alpha){}^3\text{H}$ spectrum is plotted in momentum coordinates as in Fig. 3, then the separation between the peaks is $2\Delta p$, corresponding to the relative angular momentum of the α - t clusters. Using the observed value of $\Delta p = 53 \text{ MeV}/c$ gives a measure of the separation, $R_{\alpha-t} = \hbar/\Delta p = 3.7 \text{ fm}$.

The results of ${}^6\text{Li}(\alpha, \alpha d)$ are shown in Fig. 4(a) where the sequential competition is more prominent than in the case of the $(\alpha, 2\alpha)$ spectra. Figures 4(b), 4(c), and 4(d) show the results for $x=t$, ${}^3\text{He}$, and p , respectively. All of these spectra show clear indication of QE scattering, with the exception of $(\alpha, \alpha t)$, the only one for which the free cross section is not known in the energy range of interest. (See Table I.) In addition, the $(\alpha, \alpha p)$ experiment was run at two other pairs of

QE angles in order to insure that it followed the free cross section, and also to try to improve the measurement of the shape of the distribution. As can be seen in Fig. 5, the relative cross sections followed the free cross sections quite well. Because of the high background from α particles elastically scattered from protons in the Mylar backing, measurement of the shape was not comparable with that of the other QE reactions. In this report, it should be noticed that the maximum angle of the α detector for observing QE $(\alpha, \alpha p)$ scattering is approximately 10° , which necessitated the use of quite low beam currents in an attempt to alleviate the high-background problem.

V. DISCUSSION

Applying the PWIA, it is possible to extract for each clustering possibility an experimental momentum distribution. As indicated earlier, this distribution represents the square of the Fourier transform of the radial wave function of the target nucleus. Considerable work had been done on the

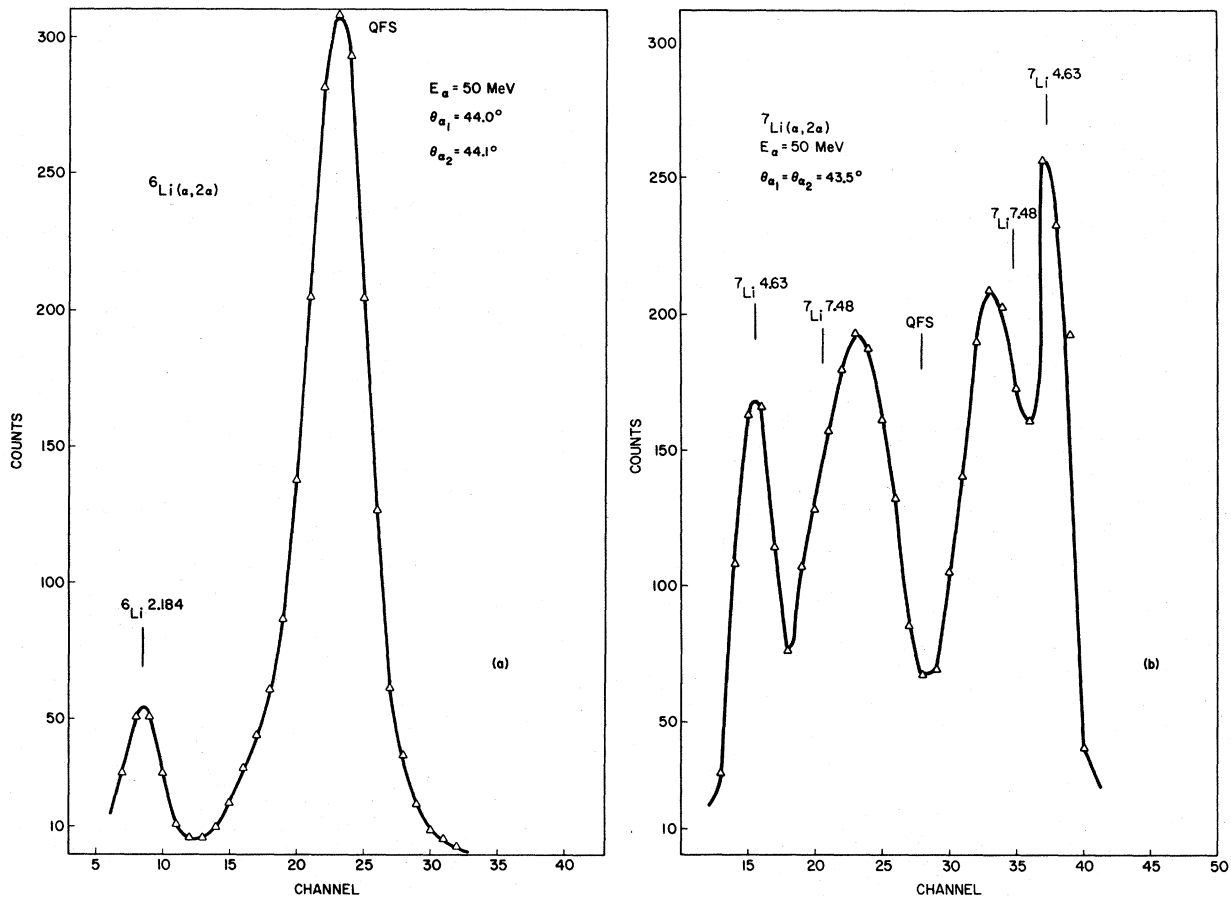


FIG. 2. Projections of kinematic locus data onto an α -particle energy axis. (a) ${}^6\text{Li}(\alpha, 2\alpha){}^3\text{H}$ and (b) ${}^7\text{Li}(\alpha, 2\alpha){}^3\text{H}$.

problem of α -particle and deuteron clustering in ${}^6\text{Li}$.^{20,27-34} Theoretical momentum distributions have been calculated using asymptotic s -state, α - d -cluster-model, shell-model, and oscillator-cluster-model wave functions. The normalization of the theoretical curve to the experimental one is, in principle, the probability of finding the target nucleus in the particular cluster configuration under consideration. Typical values obtained for α -particle and deuteron clustering probabilities in ${}^6\text{Li}$ range from 2 to 20%.

In the analysis of the present experiment, it was realized that one of the most interesting and important aspects was direct comparison of all the various quasielastic processes. In light of this, exact, detailed wave functions were ignored. Simple wave functions which could be applied in all cases but which could still reveal interesting trends in the data were used. Basically, these functions were a Gaussian of the form

$$\Psi(r) = \left(\frac{q_a^2}{\pi}\right)^{3/4} \exp\left(-\frac{1}{2}q_a^2 r^2\right), \quad (2)$$

and a Yukawa function having the form

$$\Psi(r) = \left(\frac{q_a}{2\pi}\right)^{1/2} e^{-q_a r}. \quad (3)$$

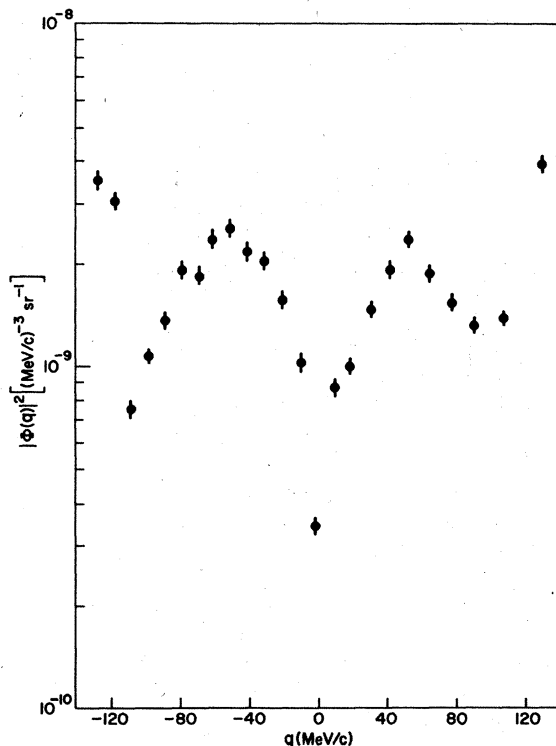


FIG. 3. The ${}^7\text{Li}(\alpha, 2\alpha){}^3\text{H}$ projection plotted as a function of recoil momentum.

The results for the $(\alpha, 2\alpha)$ and $(\alpha, \alpha d)$ experiments are shown in Fig. 6. The solid curves represent PWIA calculations, using simple Gaussians, normalized to the data. Measurements of the full width at half maximum (FWHM) and the normalization factors are listed in Table II. There is a noticeable shift of both the $(\alpha, 2\alpha)$ and the $(\alpha, \alpha d)$

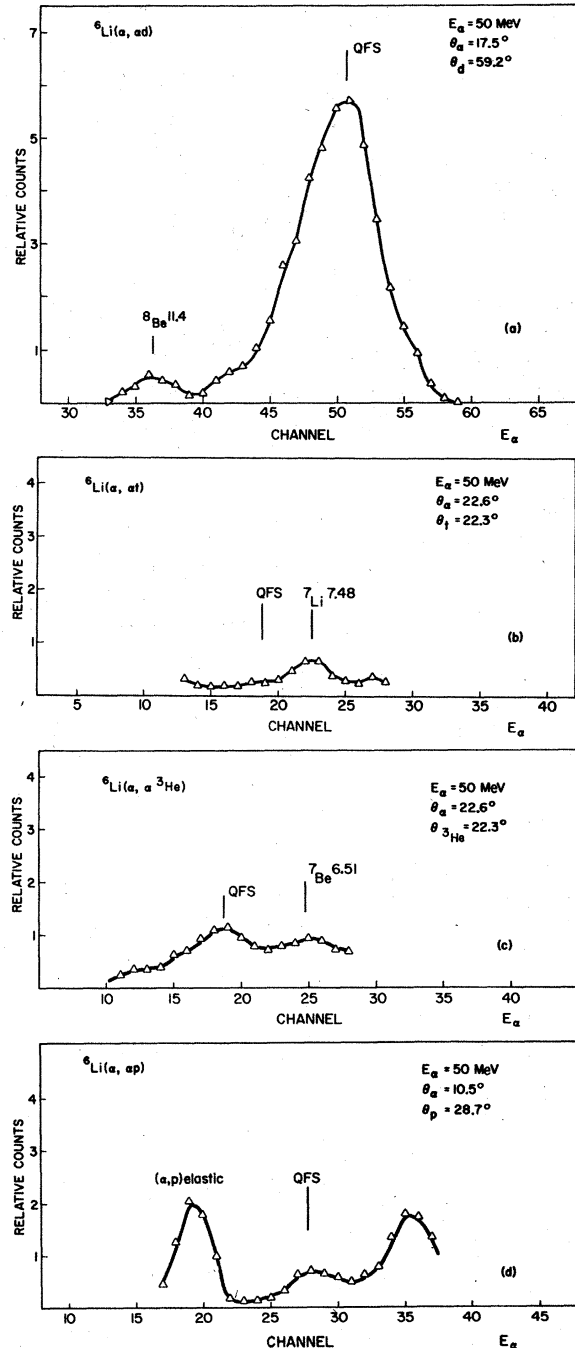


FIG. 4. (a)–(d) Examples of quasielastic scattering data for different cluster configurations.

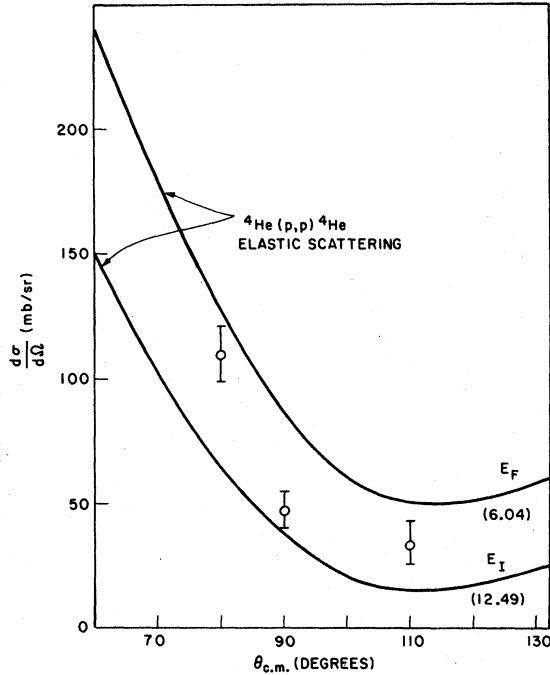


FIG. 5. Comparison of the experimental $(\alpha, \alpha p)$ quasi-elastic scattering cross section ($d^2\sigma/d\Omega^2$) and the α - p elastic scattering cross section for both the initial- and the final-state relative energy as a function of c.m. scattering angle. The solid curves represent the elastic cross section and the open circles the quasielastic. Normalization is arbitrary.

peaks with respect to the $q=0$ point. This shift, which is not predicted by the PWIA, has been attributed to a long-range Coulomb interaction between the incoming α particle and the spectator.³⁵ It should be pointed out that the normalization factors of clustering probabilities are almost identical for $(\alpha, 2\alpha)$ and $(\alpha, \alpha d)$, as one would expect if α - d

is a valid cluster configuration for the ${}^6\text{Li}$ ground state.

It is not possible to compare the $(\alpha, \alpha t)$ and $(\alpha, \alpha {}^3\text{He})$ data in the same manner as the $(\alpha, 2\alpha)$ and $(\alpha, \alpha d)$ data. Although there is a small $(\alpha, \alpha {}^3\text{He})$ contribution, the $(\alpha, \alpha t)$ configuration appears to be almost nonexistent. An interpretation of this phenomenon can not be made until more is known about the α -triton elastic scattering cross sections in this energy region. The data for these two experiments were obtained simultaneously at the same angles. This was possible, since the only kinematic difference between the two reactions is the small ${}^3\text{He}$ - t mass difference. As explained earlier, all parts of this experiment were performed under the restriction that the spectator be a single particle or cluster in its ground state. This means that when a ${}^3\text{He}$ particle is quasielastically scattered from a ${}^6\text{Li}$ nucleus, the spectator is a triton, not two neutrons plus a proton or a neutron plus a deuteron. There must be true t - ${}^3\text{He}$ clustering. Thus, if one is to reconcile the $(\alpha, \alpha t)$ and $(\alpha, \alpha {}^3\text{He})$ data and obtain equal normalization factors in the frame work of the PWIA, the α - t elastic scattering cross sections must be considerably different at the particular angle and energy used in this experiment.

The results for the $(\alpha, \alpha {}^3\text{He})$ experiment are shown in Fig. 7. The width of the $(\alpha, \alpha {}^3\text{He})$ momentum distribution is somewhat narrower than the $(\alpha, 2\alpha)$ distribution. This fact is in agreement with the findings of Bachelier *et al.*³⁶ which indicated qualitatively that the $(p, p {}^3\text{He})$ momentum distribution was narrower than that of the $(p, p\alpha)$. The over-all shape of the $(\alpha, \alpha {}^3\text{He})$ distribution is that of a relative $l=0$ configuration for the t and ${}^3\text{He}$ particles in ${}^6\text{Li}$. Direct comparison of the $(\alpha, 2\alpha)$ and $(\alpha, \alpha {}^3\text{He})$ data indicates relatively little ${}^3\text{He}$ - t clustering in the ${}^6\text{Li}$ ground state. Analysis of

TABLE II. Results of width measurements and normalization factors for theoretical fits to the experimental data.

Reaction	Width (FWHM) (MeV/c)	Wave function	Normalization (units of 10^{-2})
${}^6\text{Li}(\alpha, 2\alpha)$	57	A ^a	0.95
		B ^b	16
		C ^c	82
${}^6\text{Li}(\alpha, \alpha d)$	62	A	1.1
		B	8.7
		C	30
${}^6\text{Li}(\alpha, \alpha {}^3\text{He})$	44	A	0.001
		B	0.06
${}^6\text{Li}(\alpha, \alpha p)$	44	A	0.10
		B	1.10

^a Gaussian.

^b Asymptotic or Yukawa function with the correct binding energy and no cutoff.

^c Yukawa function with the correct binding energy and a 5-fm cutoff.

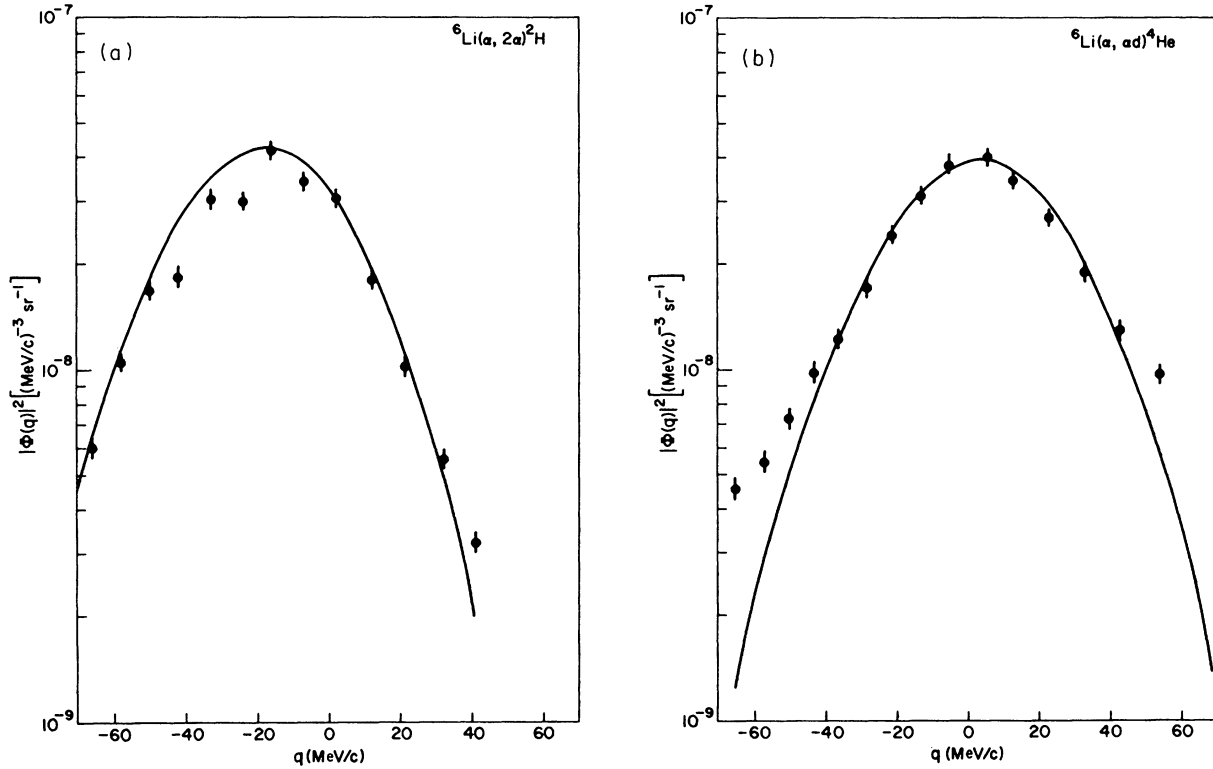


FIG. 6. The $(\alpha, 2\alpha)$ and $(\alpha, \alpha d)$ experimental momentum distributions. The solid curves are theoretical fits calculated using simple Gaussians. (a) ${}^6\text{Li}(\alpha, 2\alpha){}^2\text{H}$ and (b) ${}^6\text{Li}(\alpha, \alpha d){}^4\text{He}$.

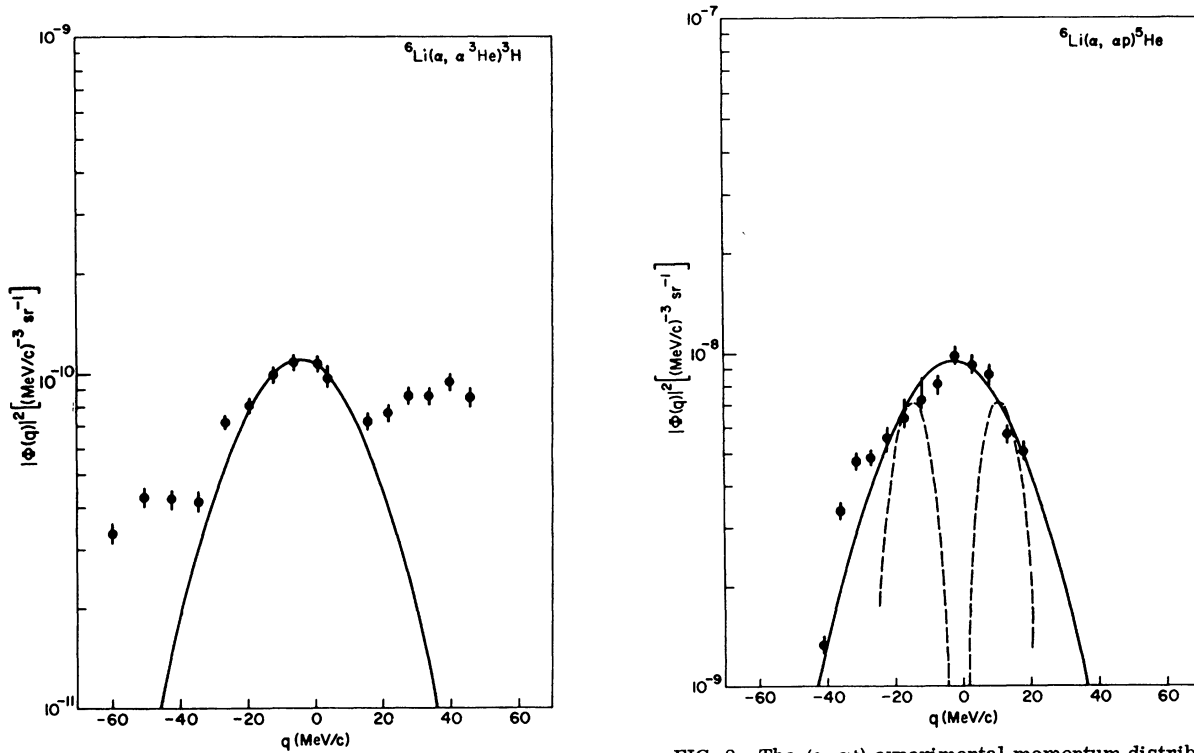


FIG. 7. The $(\alpha, \alpha {}^3\text{He})$ experimental momentum distribution. The solid curve is a PWIA theoretical fit.

FIG. 8. The $(\alpha, \alpha p)$ experimental momentum distribution. The solid curve represents the PWIA $l=0$ theoretical fit, while the dashed curve represents the PWIA $l=1$ fit.

data^{37,38} from the reaction ${}^7\text{Li}({}^3\text{He}, \alpha){}^6\text{Li}$ in terms of exchange mechanisms has suggested that there is a finite probability of ${}^6\text{Li}$ existing in a ${}^3\text{He}+t$ configuration. The results of the present experiment confirm the existence of this finite probability but disagree with recent estimates³⁹ of the amount of ${}^3\text{He}-t$ clustering based upon analysis of data on the direct radiative capture of ${}^3\text{He}$ by tritons. However, such estimates employ radial wave functions generated by a single-channel resonating-group calculation which ignores the possibility of $\alpha+d$ clustering. The present experiment, on the other hand, considers all possibilities and measures them in essentially the same manner.

The $(\alpha, \alpha p)$ results are also shown in Fig. 8. Although the statistics are poor for reasons discussed previously, the momentum distribution appears to reach a maximum at $q=0$ rather than a minimum. This may imply a strong $l=0$ contribution to this process not expected from shell-model considerations. For this particular case, both $l=0$ and $l=1$ wave functions are shown with the data. The widths of these functions were chosen so as to be consistent with the experimental results. The FWHM for the $l=0$ curve, as shown in Table II, is narrower than that of the $(\alpha, 2\alpha)$ data. The width of the $l=1$ curve yields a mea-

sure of the cluster separation, $R_{p-{}^5\text{He}} \cong \hbar/\Delta p \cong 16$ fm.

The above results seem to indicate the same conclusions concerning the shell model as the early $(p, 2p)$ experiments on ${}^6\text{Li}$. The experimental momentum distribution appears to have a shape consistent with $l=0$ relative orbital angular momentum for the $p-{}^5\text{He}$ system. Based upon spin and parity arguments and our knowledge of ${}^5\text{He}$, this should not be so. If, however, this is really an $l=1$ distribution with the minimum filled in or masked over, the narrowness of the distribution indicates a nuclear size somewhat inconsistent with the shell model.

It is known that the binding-energy tail of the wave function plays an important role and can cause substantial variations in all phases of theoretical calculations. Figure 9 illustrates the variation of the magnitude and shape of momentum distributions calculated for a Yukawa or asymptotic function versus q_a . The parameter q_a can be expressed as a function of the binding energy of the knocked-out cluster in the target nucleus through the two equations:

$$q_a = (2m_\alpha \epsilon)^{1/2}, \quad (4)$$

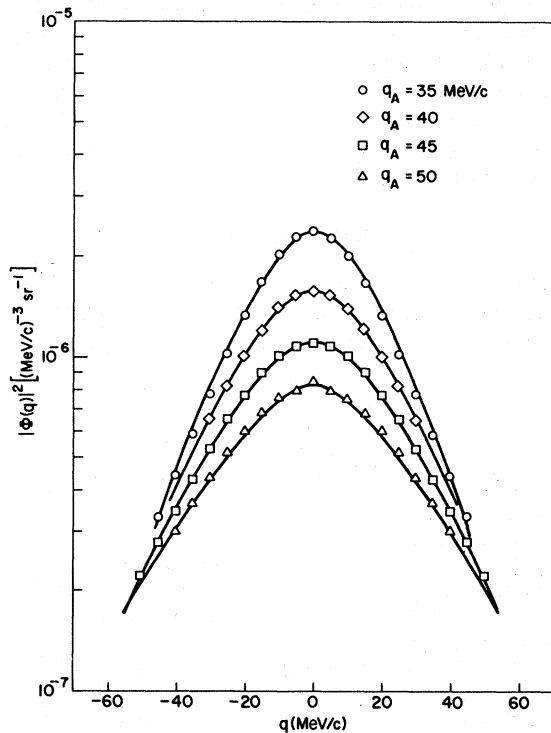


FIG. 9. Variation of the magnitude and shape of momentum distributions calculated for a Yukawa function versus the parameter q_a .

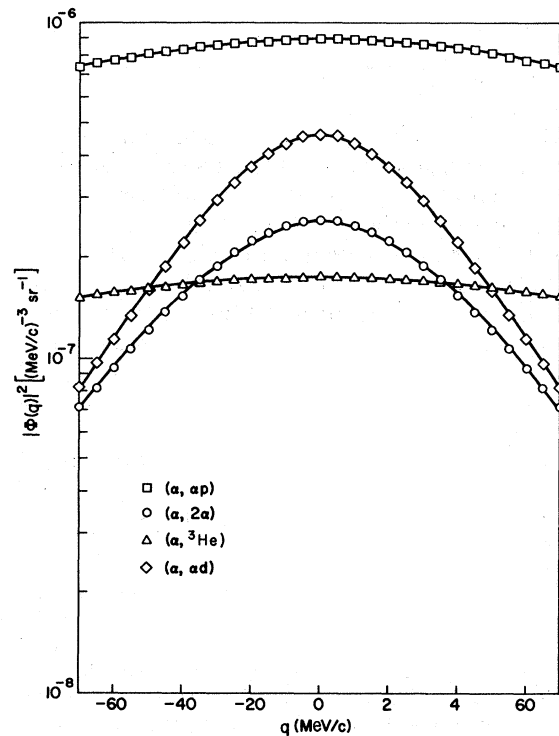


FIG. 10. Theoretical momentum distributions for $p, d, {}^3\text{He}$, and α -cluster knockout calculated using correct binding energies.

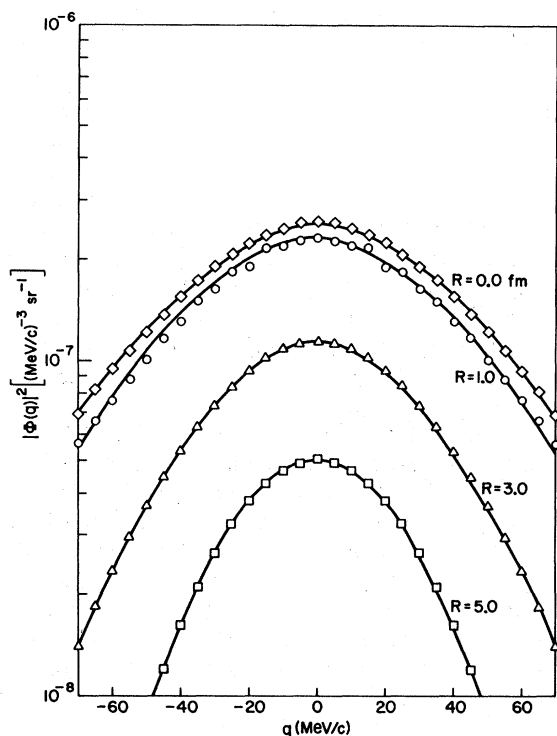


FIG. 11. Theoretical $(\alpha, 2\alpha)$ momentum distributions calculated using a Yukawa function with the correct binding energy. The different curves are for different cutoff radii.

$$\epsilon = E_B / \left(1 + \frac{m_\alpha}{m_x} \right). \quad (5)$$

In these equations m_α and m_x are the mass of the α particle and the mass of the knocked-out particle, respectively; ϵ is the "reduced" binding energy; and E_B is the true binding energy. Figure 10 shows the momentum distributions calculated with the correct binding energy for p , d , ${}^3\text{He}$, and α knockout. Comparison of Figs. 9 and 10 indicates that in order to fit the shape of each distri-

bution the true binding energy, E_B , must be reduced from its known value. In all cases, however, the Yukawa function gives better agreement in magnitude between theory and experiment than a simple Gaussian; the agreement is much better in cases in which the correct binding energy is used.

At low bombarding energies absorption and distortion effects are major problems. It has been found that these effects along with a form of localization of the interaction can be parametrized by the introduction of a cutoff radius in the wave function. Figure 11 shows the behavior of the correct-binding-energy Yukawa function for $(\alpha, 2\alpha)$ scattering as a function of the cutoff radius. Normalization factors are given in Table II for all cases treated.

In conclusion, it can be said that quasielastic scattering can be used successfully as a tool in studying the cluster structure of the light nuclei. Considering the basic purpose of the present experiment, analysis of the data in the framework of the PWIA utilizing relatively simple functions is justified and has served to point out several interesting facts. Even at these energies, the PWIA proves to be a fair approximation with several obvious discrepancies. The necessity of introducing asymptotic functions and radial cutoffs indicates that clustering is an extremely surface-oriented phenomenon. Finally, absolute clustering probabilities can not be obtained in this naive approach but good relative indications can. Absolute probabilities are extremely sensitive to the form of the wave function. Relative probabilities indicate that ${}^6\text{Li}$ has strong p , d , and α clustering and rather weak t and ${}^3\text{He}$ clustering.

ACKNOWLEDGMENTS

The authors are grateful for the support of the cyclotron operations staff and to Dr. Rollon O. Bondelid for his constant interest and support.

*Permanent address: Georgetown University, Washington, D. C.

†NAS-NRC Resident Research Associate at the Naval Research Laboratory.

¹Rev. Mod. Phys. **37**, 327 (1965).

²Proceedings of the International Conference on Clustering Phenomena in Nuclei, Bochum, Germany, 1969 (International Atomic Energy Agency, Vienna, Austria, 1969).

³J. M. Lambert, P. A. Treado, L. A. Beach, R. B. Theus, and E. L. Petersen, Nucl. Phys. **A152**, 516 (1970).

⁴A. W. Parker, J. S. Allen, R. L. Yerke, and V. G. Shotland, Phys. Rev. **174**, 1093 (1968).

⁵C. Moazed and H. D. Holmgren, Phys. Rev. **166**, 977 (1968).

⁶M. A. Waggoner, J. E. Etter, H. D. Holmgren, and

C. Moazed, Nucl. Phys. **88**, 81 (1966).

⁷J. D. Bronson, W. D. Simpson, W. R. Jackson, and G. C. Phillips, Nucl. Phys. **68**, 241 (1964).

⁸P. G. Roos, H. G. Pugh, M. Jain, H. D. Holmgren, and M. Epstein, Phys. Rev. **176**, 1246 (1968).

⁹M. Epstein, H. D. Holmgren, M. Jain, H. G. Pugh, P. G. Roos, N. S. Wall, C. D. Goodman, and C. A. Ludemann, Phys. Rev. **178**, 1698 (1969).

¹⁰A. N. James and H. G. Pugh, Nucl. Phys. **42**, 441 (1965).

¹¹J. M. Lambert, R. J. Kane, P. A. Treado, L. A. Beach, R. B. Theus, and E. L. Petersen, Bull. Am. Phys. Soc. **15**, 1694 (1970).

¹²J. P. Garron, J. C. Jacmart, N. Riou, and Ch. Ruhla, J. Phys. Radium **22**, 622 (1961).

- ¹³J. P. Garron, J. C. Jacmart, M. Riou, C. Ruhla, J. Teillac, and K. Strauch, Nucl. Phys. 37, 126 (1962).
- ¹⁴H. Tyrén, S. Kullander, O. Sundberg, R. Ramachandran, and P. Isacsson, and T. Berggren, Nucl. Phys. 79, 321 (1966).
- ¹⁵J. C. Roynette, M. Arditi, J. C. Jacmart, F. Mazloum, M. Riou, and C. Ruhla, Nucl. Phys. A95, 545 (1967).
- ¹⁶D. R. Inglis, Rev. Mod. Phys. 34, 165 (1962).
- ¹⁷P. G. Roos, H. Kim, M. Jain, and H. D. Holmgren, Phys. Rev. Letters 22, 242 (1969).
- ¹⁸G. Paic, J. C. Young, and D. J. Margaziotis, Phys. Letters 32B, 437 (1970).
- ¹⁹H. G. Pugh, J. W. Watson, D. A. Goldberg, P. G. Roos, D. I. Bonbright, and R. A. J. Riddle, Phys. Letters 22, 408 (1969).
- ²⁰J. W. Watson, Ph.D. thesis, University of Maryland, 1970 (unpublished).
- ²¹T. Berggren, G. E. Brown, and G. Jacob, Phys. Letters 1, 88 (1962).
- ²²T. Berggren and G. Jacob, Phys. Letters 1, 258 (1962).
- ²³T. Berggren and G. Jacob, Nucl. Phys. 47, 481 (1963).
- ²⁴C. Zupānčić, *Les Réactions Nucléaires à Trois Corps* (Institut de physique nucléaire de Université de Lausanne, Lausanne, Switzerland, 1967), p. 42.
- ²⁵P. Gaillard, M. Chevallier, J. Y. Grossiord, A. Guichard, M. Gusakow, J. R. Pizzi, and J. P. Maillard, Phys. Rev. Letters 25, 593 (1970).
- ²⁶D. I. Bonbright, private communication.
- ²⁷J. R. Pizzi, M. Gaillard, P. Gaillard, A. Guichard, M. Gusakow, G. Reboulet, and C. Ruhla, Nucl. Phys. A136, 496 (1969).
- ²⁸M. Jain, Ph.D. thesis, University of Maryland, 1969 (unpublished).
- ²⁹V. K. Dolinov, Yu. V. Melikov, A. F. Tulinov, and O. V. Bormot, Nucl. Phys. A129, 577 (1969).
- ³⁰D. L. Hendrie, University of California Radiation Laboratory Report No. UCRL 16580, 1966 (unpublished).
- ³¹A. D. Bacher, Bull. Am. Phys. Soc. 14, 534 (1969).
- ³²D. W. Devins, B. L. Scott, and H. H. Forster, Rev. Mod. Phys. 37, 396 (1965).
- ³³C. Ruhla, M. Riou, J. P. Garron, J. C. Jacmart, and L. Massonnet, Phys. Letters 2, 44 (1962).
- ³⁴C. Ruhla, M. Riou, M. Gusakow, J. C. Jacmart, M. Liu, and L. Valentin, Phys. Letters 6, 282 (1963).
- ³⁵K. Bähr, T. Becker, O. M. Bilaniuk, and J. Jahr, Phys. Rev. 178, 1706 (1969); P. A. Assimakopoulos, E. Beardsworth, D. P. Boyd, and P. F. Donovan, Nucl. Phys. A144, 272 (1970).
- ³⁶D. Bachelier, M. Bernas, C. Détraz, P. Radvanyi, and M. Roy, Phys. Letters 26B, 283 (1969).
- ³⁷P. D. Forsyth and R. R. Perry, Nucl. Phys. 67, 517 (1965).
- ³⁸A. R. Knudson and E. A. Wolicki, in *Proceedings of the Conference on Direct Interactions and Nuclear Reaction Mechanisms, Padua, 1962* (Gordon and Breach, New York, 1963), p. 981.
- ³⁹A. M. Young, S. L. Blatt, and R. G. Seyler, Phys. Letters 25, 1764 (1970).